

Stable Forward Dynamic Simulation of Bipedal Gait Using Space-Time Analysis

Granata, K.P.^{*} Brogan, D.C.[#] Sheth, P.N.[†]

Motion Analysis and Motor Performance Laboratory

^{*} Departments of Orthopaedic Surgery and Biomedical Engineering

[#] Department of Computer Science

[†] Department of Mechanical and Aerospace Engineering

University of Virginia

Keywords: Bipedal Gait, Simulation, Stability

ABSTRACT

Within the biomechanist community, there is a rhetorical hypothesis that both movement trajectory and joint torque are modulated or adapted to maintain dynamic stability in bipedal walking. Not only are these two control variables intricately related, but such additional objectives as desired speed, stealth, endurance, etc. inevitably contribute to the complex behavior in animal locomotion. As a consequence, any single objective function used to describe walking dynamics is necessarily limited. We propose a bipedal walking control algorithm that simultaneously solves for movement trajectory and joint torque without relying on any a priori assumptions regarding one or the other. The absence of such assumptions permits the study of pathologic movement dysfunctions where the desired movements and torques are unknown. Our technique uses a constraint-based space-time optimization algorithm to compute optimal movements and torques. Such pathologic constraints as leg-length discrepancy, range-of-motion limitations, or velocity constraints from spastic hypertonia may be added and this optimization technique will find non-homogeneous solutions. When this technique is applied to a control task with a known optimal solution, two-segment downhill walking, it produces identical results to a torque-free forward-integration approach. Solutions to pathologic behavior conditions were also demonstrated by limiting swing leg velocities to simulate the neuro-physiologic constraints of hamstring spasticity.

INTRODUCTION

Criteria for successful bipedal walking include both periodicity and stability^{8,9}. Except for the constraints imposed by periodicity and stability, successful walking does not require specific movement trajectories or joint torques. Hence, individuals whose joint torques are affected by neuromuscular pathology may be able to modify their movement trajectories to successfully achieve stable walking behavior in the presence of the kinematic or control constraints^{12,18}. To simulate the generalized nature of walking performance and to permit potential investigation of pathologic movement it is desirable to avoid establishing a priori the joint actuation behavior or movement trajectories. Instead one might perform a simultaneous search for joint actuation and movement trajectories constrained by periodicity and stability. The goal of the current study is to implement a simulation of bipedal walking that determines the movement trajectory simultaneously with the optimum activation torques, thereby allowing both the joint torques and movement trajectories to be modified as befitting the environmental constraints and objectives.

A simple paradigm for investigating the stability criteria in bipedal walking is the passive dynamic walker wherein a two-segment knee-less walker is driven solely by gravitational potential energy as it walks downhill²¹. Kinetic energy is lost with each foot-strike and is balanced by potential energy gained as the system moves downhill. The remarkable aspect of the passive walkers is that they can generate stable walking behavior even in the presence of disturbing forces without need for explicit controlling actuators or active feedback^{9,21,23}. A natural behavior exists such that any movement trajectory within the basin of attraction representing the stability region will converge to the preferred movement pattern^{4,10}. However, existing locomotion optimization models search for open-ended movement trajectories. These open-ended movement trajectories present technical limitations when attempting to identify stable movement trajectories.

Stability of passive dynamic bipedal walkers has been studied under a variety of conditions. Stability analyses have been performed in these compass-gait models using effective two-mass⁴ and three-mass systems^{11,23} as well as investigations into passive walking with knees^{5,22}. These seminal analyses investigate stability by means of post priori numerical computation. For

example, during passive-dynamic walking the downhill ground slope and mass distribution of the walker completely dictate stable movement trajectory. Governing equations for the movement dynamics include both non-linear differential equations to represent swing phase and algebraic discontinuities to represent foot-strike. Hence, by means of forward-integration the full movement trajectory can be specified and evolve from initial conditions. Upon completion of a complete gait cycle the trajectory can be tested for periodicity and stability^{15,16}. Consequently, when using standard methods of forward-integration it is difficult to identify the appropriate initial trajectory that will ultimately result in stability, i.e. it is unknown whether the initial conditions are appropriate until after the gait cycle is completed. Identifying stable initial conditions has been achieved by trial-and-error estimation, by linear-approximation⁴ and by Newton search methods²¹. Recognizing this limitation it is difficult to extend these models to active walking because one cannot determine the influence of an applied joint torque upon limit-cycle stability until long after the gait cycle is completed. Consequently most dynamic simulations of bipedal walking pre-specify either movement trajectories, i.e. inverse dynamic analyses, or joint actuation torques, i.e. forward-dynamic analyses. In the case of passive-dynamic walking the joint actuation torques are pre-specified as a value of zero throughout the entire gait cycle. Nonetheless, the passive-dynamic walking presents an excellent paradigm for the investigation of dynamic stability.

Recent advances in computational methods permit one to search for combinations of movement trajectories and joint actuation torques that satisfy the equations of motion, periodicity and limit-cycle stability. Conceptually, periodicity and momentum requirements describe the relation between the initial and final trajectory points for each step in symmetric gait behavior¹⁷ while the equations of motion describe the shape of the trajectory in between these initial and final points. Stability constrains the relation between joint torque and movement trajectory. Asymmetric behaviors typical in pathologic gait can likewise be established albeit through greater model complexity to permit generality. The specific aim of the current study was to determine whether these trajectory-searching algorithms allow the simulation to identify the optimum movement path that converges to stable bipedal dynamics.

A trajectory-searching algorithm known as “space-time constraints²⁹” was employed to identify stable movement trajectories in passive bipedal walking. We use a forward-dynamic simulation to generate a time-sequenced movement trajectory, which we evaluate in its entirety. A force-minimizing search algorithm identifies an optimal trajectory that implicitly establishes dynamic stability and converges to passive walking in downhill conditions. Previous simulations have pre-specified movement trajectory and require the actuation torques to control maintain that movement pattern^{2,26,28}. Others have pre-specified the actuation torques then solved for the resulting movement trajectory^{7,13,19,24,25}. Some advanced models have derived input joint torques from measured EMG data²⁷. Passive –dynamic walking requires homogeneous behavior or zero torque actuation from which movement trajectories are determined^{3,4,20}. The goal of the current study was to implement a simulation determines the movement trajectory simultaneously with the optimum activation torques, thereby allowing both the joint torques and movement trajectory to be modified as befitting the environmental constraints and objectives. To investigate the validity of the solutions results were compared with the natural behavior of passive bipedal walking. Finally, active bipedal walking was investigated, using the trajectory search simulation of compass-gait to seek movement and torque solution to level-ground and uphill walking wherein passive bipedal gait cannot exist. Significant insight into the control and stability of bipedal locomotion is established with potential applications for representing physically constrained or pathologic walking biomechanics.

METHODS

The simulation represents a 2-dimensional knee-less walker including two legs of mass m_L , joined by a revolute joint at the point mass of the head-arms-trunk (HAT), M_H and is based upon successful walking models published elsewhere^{3,4,21}. Leg masses, m_L , are located at a distance d_{CM} from the hip along a line joining the hip to the point-foot. The walker moves along a plane of slope γ with respect to horizontal. A time-dependent vector $\boldsymbol{\theta} = [\theta_S, \theta_N]^T$ represents the walker configuration where θ_S and θ_N are the angles of the stance-leg and non-stance-leg versus ground normal. During walking only one foot is in contact with the ground at any time, i.e. single-stance. Ground clearance of the swing-leg is ignored in this treatment because simple mechanisms such as prismatic joints¹¹ are readily established that do not influence walker dynamics. The governing equations of motion include the differential equations of movement

that model swing phase dynamics and the conservation of angular momentum that models foot-strike transitions. These models are implemented using classical homogeneous forward-integration techniques.

Governing Equations of Motion

The collision at foot-strike is represented with no slip and no bounce and the transition stage at foot-strike is assumed instantaneous, i.e. no double-support period¹⁷. The configuration after foot-strike θ^+ is related to the pre-impact angles θ^- by an anti-symmetric matrix, J , that establishes the new swing leg at the angle of the previous stance leg and the new stance leg with the configuration of the previous swing leg angle. Angular velocities before and after foot strike are related by conservation of angular momentum,

$$Q^+(\theta) \dot{\theta}^+ = Q^-(\theta) \dot{\theta}^- \quad (1)$$

The terms $Q^+(\theta)$ and $Q^-(\theta)$ represent the momentum matrices immediately before and after foot-strike about the forward contact foot.

$$Q^-(\theta) = \begin{bmatrix} - (1-\beta)\beta - \{2 (1-\beta)+1\}\{R_N u_N\} \times \{R'_S u_S\} & - (1-\beta)\beta \\ - (1-\beta) & 0 \end{bmatrix} \quad (2)$$

$$Q^+(\theta) = \begin{bmatrix} \beta^2 + \beta \{R_N u_N\} \times \{R'_S u_S\} & 2 (1-\beta) + \beta^2 + 1 + \beta \{R_S u_S\} \times \{R'_N u_N\} \\ \beta & \{R_S u_S\} \times \{R'_N u_N\} \end{bmatrix} \quad (3)$$

where R_S and R_N are the Euler rotation matrices for the stance leg and non-stance leg at angles θ_S and θ_N respectively and \times represents the vector, or cross-product, operator. The vectors u_S and u_N represent the unit vector directions of the stance leg and non-stance leg in a neutral configuration, $\beta = m_L/M_H$ is the mass ratio and $\beta = d_{CM}/L$ the mass-distribution ratio. Hence, state of the system immediately prior to foot contact, $\mathbf{q}^- = [\theta^-, \dot{\theta}^-]^T$ is related to the state immediately following foot-contact, $\mathbf{q}^+ = [\theta^+, \dot{\theta}^+]^T$ by the relation,

$$\mathbf{q}^+ = \begin{bmatrix} J & 0 \\ 0 & \text{inv}(Q^+) Q^- \end{bmatrix} \mathbf{q}^- \quad (4)$$

These conservation laws lead to discontinuous change in segment rotational velocities and associated kinetic energy loss at each foot-strike. Goswami et al.¹⁰ illustrate that this energy loss is necessary to maintain dynamic stability through phase-space contraction.

The equations of movement dynamics are described by classical rigid body mechanics. Because the system is continually in swing-phase it is represented as a double-pendulum with pivot at the stance foot. The dynamics are determined from two coupled, second-order differential equations of motion.

$$M(\theta)\ddot{\theta} + N(\theta, \dot{\theta})\dot{\theta} + G(\theta, \gamma) = \tau \quad (5)$$

$$M(\theta) = \begin{bmatrix} \beta \{R'_S u_S\} \{R'_N u_N\} & \beta \{R'_S u_S\} \{R'_N u_N\} \\ \beta \{R'_S u_S\} \{R'_N u_N\} & \beta^2 \end{bmatrix} \quad (6)$$

$$N(\theta, \dot{\theta}) = \begin{bmatrix} 0 & \beta \{R'_S u_S\} \{R''_N u_N\} \dot{\theta}_N \\ \beta \{R'_S u_S\} \{R'_N u_N\} \dot{\theta}_S & 0 \end{bmatrix} \quad (7)$$

$$G(\theta) = \frac{g}{L} \begin{bmatrix} (2 + \beta + 1) \{R'_S u_S\} \{R_g u_g\} \\ \beta \{R'_N u_N\} \{R_g u_g\} \end{bmatrix} \quad (8)$$

where R_S and R_N are described above, R_g is the Euler rotation matrices for the ground slope at angle γ ; and R'_S, R'_N the spatial derivatives of the rotation matrices. The vector u_g represents the unit vector directions of the gravity vectors and g the gravitational constant. The actuation vector includes terms describing the joint torques from the ankle and hip, $\tau = [\tau_A, \tau_H]^T$. To represent passive walking these joint torques must be zero. Evaluation of the motion equations reveals that the passive movement trajectories are fully determined by the ground slope, γ , the mass ratio and the mass-distribution ratio of β ¹⁰

Forward-Integration Model

The equations of dynamics are implemented on a PC using an ordinary differential equation (ODE) solver in MATLAB. Specifically, the movement trajectory is determined by means of

forward integration of the differential equations while assuming a homogeneous solution, i.e. $\tau = 0$ in the passive walker. The trajectory is monitored to identify foot-strike events by zero-crossing algorithms representing the time and state when the swing foot intersected the ground plane. The swing-foot typically intersects the ground twice, once with the leg moving up-and-

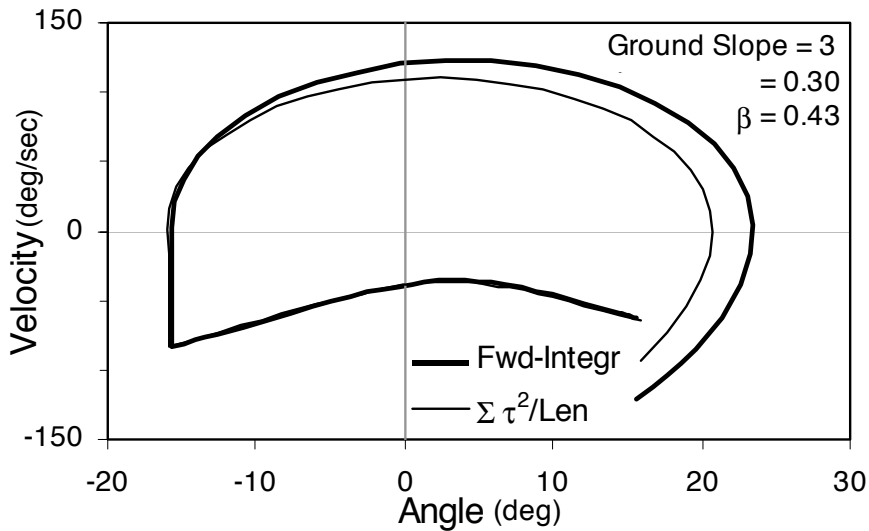


Figure 1: Phase plane representation of the movement trajectory from the simulation of the passive bipedal walker. Moving in a clockwise direction starting from the lower right quadrant, the stance leg moves from its initial state to opposite leg foot-strike occurring in the lower left quadrant. A discontinuity in velocity (equation 4) is observed as the stance leg becomes the swing leg. During swing phase the leg traversing from the left side of the plane returning to the lower left quadrant. At foot-strike the discontinuity is again noted when the swing leg transitions back into stance.

forward and again as the pendulum behavior causes it to peak and swing back. These have been described as the short-step and long-step behaviors^{5,6}. We investigate only the long-step solution as McGeer²¹ concludes the short-step is unstable. At foot-strike, the transition equation (eqn 4) is applied to re-set the state vector, \mathbf{q} . With the new configuration and velocities, the forward-dynamic ODE process is repeated to simulate the next step. The process continues for as many walking steps as necessary. Figure 1 illustrates a phase plane portrait of a typical behavior in passive downhill walking.

Analysis of limit cycle stability for the forward-integration model is performed numerically as described in the literature^{9,23}. The initial state of the system at step k results from the dynamics following from the initial state at step $k-1$. This relation has been called the “stride function”¹,

$$\mathbf{q}_k = f(\mathbf{q}_{k-1}) \quad (9)$$

If the state is perturbed $\Delta\mathbf{q}$ then a Taylor series representation of the response is described as

$$f(\mathbf{q}_{k-1} + \Delta\mathbf{q}) = \mathbf{q}_k + \nabla f \Delta\mathbf{q} \quad (10)$$

where ∇f is the gradient of the stride function with respect to the system states^{9,23}. The resultant trajectory returns toward the stable behavior only if the eigenvalues of ∇f about \mathbf{q}_k are less than one. By introducing a perturbation $\Delta\mathbf{q}$ to each of the state variables at \mathbf{q}_{k-1} and observing the response \mathbf{q}_k a numeric representation of ∇f is achieved⁴. For example, eigenvalues of the system described in figure 2 were determined as $0.290 - i 0.623$, $0.290 + i 0.623$, 0.000 , 0.068 . All are within the unit circle indicating a stable movement trajectory. Stability analyses are performed in this manner for all conditions.

Constrained Trajectory Search Model

We also implemented the two-legged walker using space-time constraints to solve for the movement trajectories and joint torques. This model is identical to the system described above in terms of equations of dynamics and foot-strike transition, but a linear-search algorithm is used to identify the optimum trajectories of the entire movement rather than time incremental forward integration. The advantage of the trajectory search method is 1) the solution is not limited by a priori assumptions regarding the initial state, 2) the objective function can be designed to seek intrinsically stable trajectories, and 3) the solution is not limited to homogenous solutions or a priori actuation or movement behaviors thereby permitting assessment of optimal movement trajectories and joint torques for uphill walking.

The method of space-time constraint represents the movements and torques as a series of multiple piecewise linear trajectories. This permits numeric representation of the velocity and acceleration as linear functions of position. The technique for solution of forward-dynamic simulation has been described elsewhere for multi-segment reaching tasks²⁹ but has never been applied to the compass-gait problem. The entire movement trajectory is established with an angle vector $\boldsymbol{\theta}_t = [\theta_{S_t}, \theta_{N_t}]^T$ at every time increment $t = 1 \dots n$. Note that the full angle vector includes two legs at n time increments represented in a 1-by- $2n$ vector. The velocity and acceleration vectors are also 1-by- $2n$ column matrices determined by multiplying the position vector $\boldsymbol{\theta}_t$ by numeric differentiation matrices, $\dot{\boldsymbol{\theta}} = \mathbf{V} \boldsymbol{\theta}_t$ and $\ddot{\boldsymbol{\theta}} = \mathbf{A} \boldsymbol{\theta}_t$

$$\mathbf{V} = \frac{.5}{dt} \begin{bmatrix} -1 & 0 & 1 & 0 & 0 & 0 & \dots \\ 0 & -1 & 0 & -1 & 0 & 0 & \dots \\ 0 & 0 & -1 & 0 & -1 & 0 & \dots \end{bmatrix} \quad (11)$$

$$\mathbf{A} = \frac{1}{dt^2} \begin{bmatrix} 1 & -2 & 1 & 0 & 0 & 0 & \dots \\ 0 & 1 & -2 & -1 & 0 & 0 & \dots \\ 0 & 0 & 1 & -2 & -1 & 0 & \dots \end{bmatrix} \quad (12)$$

where dt is the time increment. The non-linear, second-order differential equations of motion are represented by expanding the terms $M(\theta)$, $N(\theta, \dot{\theta})$ and $G(\theta, \gamma)$ (eqns 5-8) into $2n$ -by- $2n$ matrices with coefficients determined from the state vector at each time increment. An arbitrary motion trajectory θ_t requires a set of actuation torques, $\tau_t = [\tau_{A_t}, \tau_{H_t}]^T$ to satisfy the equations of motion (eqn 5), where τ_{A_t} represents the ankle torque of the stance leg and τ_{H_t} represents the hip torque at time t . Additionally, the time-increment dt is implemented as a variable thereby allowing the swing period to approach an optimum.

Using constrained optimization routines in MATLAB it is possible to solve for the movement trajectory θ_t that minimizes the sum of squares of actuation torques throughout the stride cycle.

$$\min \sum \tau_t^T * \tau_t \quad (13)$$

where a full stride cycle is the time between consecutive foot strikes. In the special case where passive walking is simulated, one expects this sum of squares to approach zero, i.e. no actuation torque is applied to generate passive dynamic walking. Because the initial angles and step length trend toward zero as ground slope approaches horizontal^{6,11,21} we also investigate simulations using another objective function that minimizes the sum of torques while penalizing the behavior of short step lengths,

$$\min \sum (\tau_t^T * \tau_t^T) / \text{Step-Length} \quad (14)$$

Recognizing that the objective functions will identify energy wells in the movement dynamics, the search algorithm will intrinsically seek stable behavior.

Constraints to the solution space are imposed as part of the optimization routine in order to limit the solution space and to speed the convergence. These include limitations on feasible joint angles ± 90 degrees to prevent solutions wherein the walker performs flips and whirling gait

behaviors¹⁴. An upper bound on the time increment, dt , is also established to limit the total swing period less than 2π , i.e. the swing leg is not permitted to swing back-and-forth multiple times within a single step. Finally, the system state at the initial and final time-points are constrained to assure periodicity and conservation of momentum (eqn 4).

Output includes the movement trajectory, stance leg ankle torques, and inter-segment hip torques at each instant in time. Stride period is calculated from the product of the time increment dt and the number of time increments n . Step length is determined from the geometric relation involving the initial and final leg angles. Recognizing that periodicity constraints require the angles are equal and opposite between legs and at the initial and final time points, the stride length is simply:

$$\text{Stride Length} = 2*L*\sin(\theta_{Si}) \quad (15)$$

where L is the leg length and θ_{Si} the angle of the stance leg at the initial data point.

To assure the solution trajectories are stable according to the eigenvalue analyses, the results from the trajectory search are applied to the forward-integration model for comparison. Using initial conditions predicted by the trajectory search solution, the forward-integration model is allowed to iterate forward in time to establish the full movement trajectory. The trajectories predicted by these two models were compared and found to be identical for most downhill walking conditions. Eigenvalue results were therefore representative of the limit-cycle stability of trajectory search solution.

RESULTS

The forward-integration two-legged walker simulation generates steady state behavior and demonstrates notable trends in association with ground slope. To confirm steady state behavior, the forward-integration model is simulated 100 consecutive steps. The model is initialized with leg angles of $\pm 15^\circ$, stance leg velocity of 60 deg/sec and swing leg velocity of 0 deg/sec. Because this initial state is within the limit-cycle basin of attraction the behavior undergoes transient state changes in the first few steps but quickly converges within four decimal places to the steady state behavior describing the natural dynamics of the system (see figure 2). The

behavior of the system is indicated by the mean steady state value sampled at the beginning of each step, i.e. the state immediately following foot-strike.

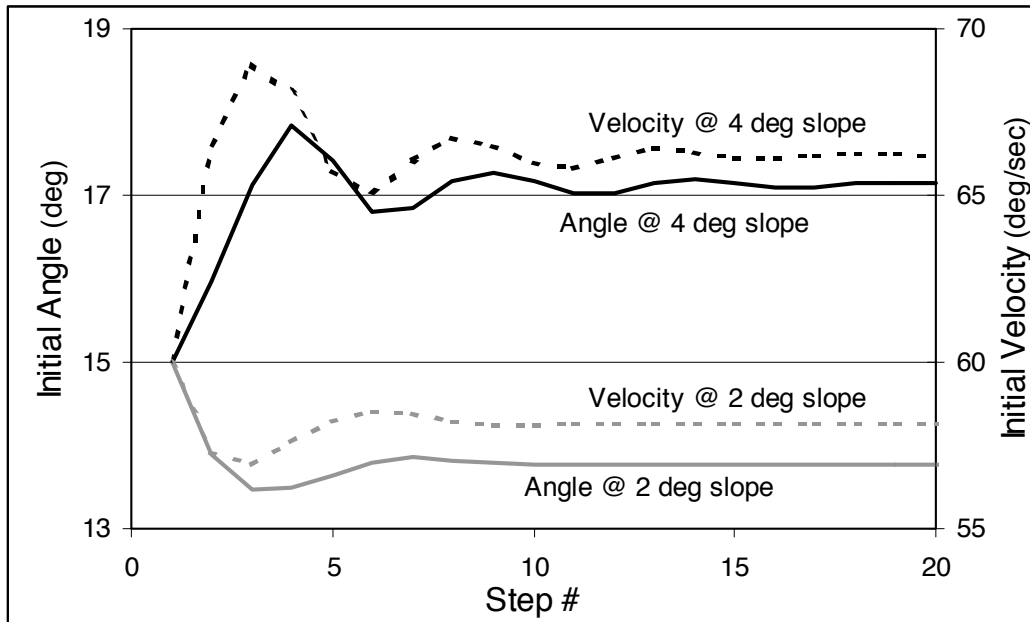


Figure 2: Transient behavior of the passive bipedal walker determined from the forward-integration model. Angle (dashed line) and velocity of the leg segments demonstrate transient changes in the first few steps but quickly converge to a stable walking behavior. Steady state behavior at each ground slope is determined by allowing the simulation to walk for 100 steps.

Steady state movement trajectories (see figure 1) are comparable to phase-plane portraits of similar systems reported in the literature^{6,11,21}. The illustrated phase-path describes the complete step trajectory of one leg. The cycle begins in stance-phase with positive stance-leg angle and negative stance-leg velocity, i.e. lower-left quadrant of the phase plane. Moving clockwise in the phase plane the stance leg reaches an angle at opposite leg foot-strike equal and opposite to the initial angle to assure periodicity. At foot-strike an instantaneous change in velocity occurs to transition the swing leg to become the swing leg. This instantaneous state change results from the conservation of momentum during the foot-strike collision and is similar to published results^{6,11,21}. The leg continues its clockwise path through the phase plane during swing phase, achieving large positive velocities until foot-strike. At ipsilateral foot-strike a second momentum-dependent velocity shift occurs to return the system to its original configuration.

The natural dynamics of the walker are strongly influenced by ground slope (see figure 2). Leg angle at foot-strike and the associated stride length increase with steeper downhill ground slope. Note that the stride length approaches zero as ground slope approaches zero. Recall that the system behaves as a pendulum and the period of a pendulum is minimally influenced by swing amplitude at the angles observed here. Hence, stride period is generally independent of ground slope, declining less than 3% as slope changes from 0.25° to 8.0° . Because step angle increases with ground slopes and stride period remains largely unchanged it is necessary for stance-leg velocity to increase with ground slope. Swing-leg velocity is negative at shallow slopes indicating the initial movement of this limb is backward or opposite the walker's direction of progression. As downhill slope increases the swing-leg velocity becomes positive, i.e. initial velocity of the swing leg is forward. As a result, the swing leg completes nearly a full pendulum cycle at shallow downhill slopes while the percent of completed cycle declines in sigmoidal fashion as with steeper slopes. Velocity of forward progression is defined as the quotient of stride length over stride period and increases with steeper downhill slopes in proportion to leg angle at foot strike. Hence, the passive walker slows and eventually stops at shallow ground slope. Clearly, the passive walker described by the forward-integration model cannot walk uphill. In fact, the maximum eigenvalue amplitude abruptly increases to unstable values as the ground slope approaches zero.

The space-time trajectory search model successfully estimates the movement trajectories for passive walking. Walker configuration is initialized at leg angles of $\pm 1^\circ$ with initial and final stance and swing leg velocities of ± 3 deg/sec and linear trajectories in between. In independent analyses the configuration is initialized at leg angles of $\pm 30^\circ$ with initial and final stance and swing leg velocities of ± 90 deg/sec and linear trajectories in between. These are selected to assure the initial conditions are well outside of the basin of attraction for the natural dynamics thereby requiring the simulation to seek a stable trajectory. Nonetheless, the simulation converges on movement trajectories that are similar to the forward-integration results. When the model solves for a trajectory that minimizes the sum of squares of the actuation torques (eqn 13), results are identical to the behavior exhibited by the forward-integration model. The trajectory successfully identifies the passive walking behavior illustrated by the fact that the sum of actuation torques approaches zero, indicating a homogeneous solution. The leg angles and

velocities are identical to the forward-integration results and therefore will not be discussed further. When the model solves for a trajectory that minimizes the sum of squares of the actuation torques per stride-length (eqn 14), results are again similar to the behavior exhibited by the forward-integration model as illustrated in the phase-portrait representation of the movement trajectories (see figure 1). In downhill walking the actuation torques approach zero, indicating the solution approximates passive walking while leg angle at foot-strike, stance-leg initial velocity and forward walking velocity increase with steeper downhill slopes as described in the forward-integration model.

Small differences are observed between the natural dynamics and the trajectories obtained from optimized joint torque per stride-length. None of these differences are statistically significant in pairwise comparisons. The leg angles at foot-strike predicted by the two methods are remarkably similar, with the trajectory search solution generating leg angles and stride lengths that are greater than the natural-dynamic behaviors by an average (\pm std) of less than $0.35^\circ \pm 0.15$. This results from the objective function that attempts to increase step length while simultaneously minimizing actuation torques. Stride lengths are $1.1\% \pm 0.5$ longer than the passive results. Deviation from the passive dynamics requires active joint torques. However, because of the close agreement between predicted and passive trajectories these actuation torques are quite small, with mean downhill levels of 0.004 rad/sec^2 . (N.B. actuation torques were normalized by system inertia thereby representing torque as applied acceleration generated by the muscles or motor actuators.) Compared to a mean natural dynamics, passive trajectories produce a stride period of 648 msec whereas the trajectory search solution produces a period that is 22 ± 18 msec slower. Consequently, the initial state velocities of the swing-leg are slightly faster in both the positive and negative directions resulting in a compensation velocity of the stance leg, with a difference of 2.7 deg/sec and 1.1 deg/sec respectively. The goal of the trajectory search simulation is to identify stable movement trajectories and actuation torques for the bipedal walker. To test the solution stability, predicted initial conditions are applied to the forward-integration model and the eigenvalue stability determined. In all downhill conditions the trajectory search model identified stable movements with eigenvalue amplitudes less than one. This is not surprising considering the initial conditions of the two models are nearly identical.

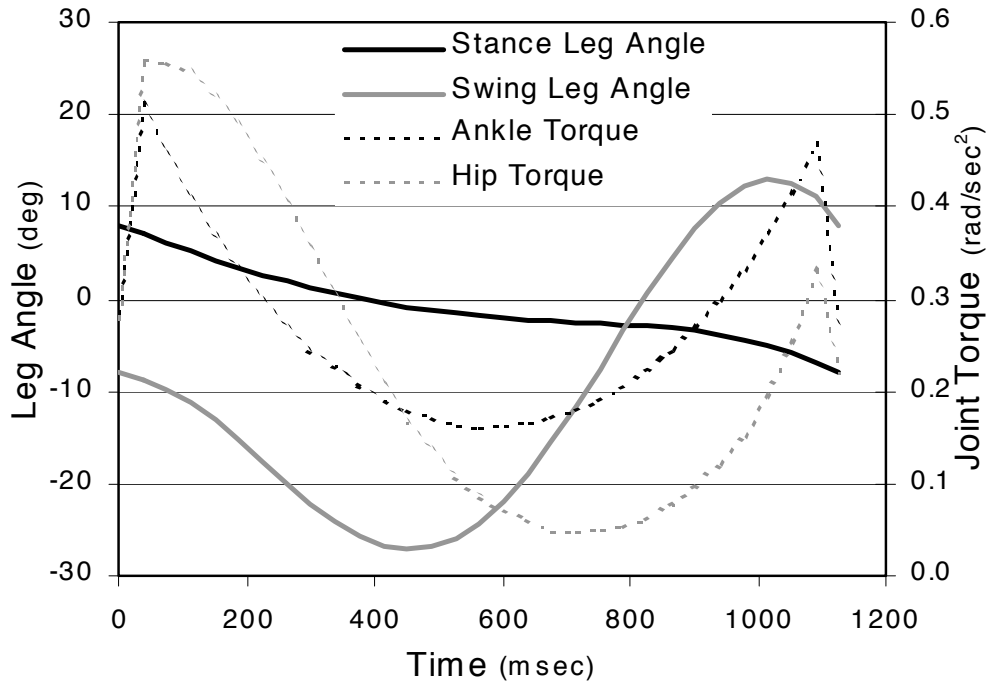


Figure 3: Walking behavior accomplished for a 2.0° uphill slope. Both the ankle and hip muscles must apply torques .

The system successfully achieves uphill walking because the objective function encourages non-zero step lengths (eqn 14). As indicated above, a homogeneous system requires the solution must approach zero step length at shallow ground slopes. Both the forward-integration model and the simulations that minimize sum of squared torques demonstrate this behavior.

Conversely, since the objective function of the last model resists zero step lengths, the movement trajectory continues to represent forward walking on uphill slopes but clearly could not achieve a homogeneous solution when walking uphill. The result is a set of time-dependent joint torques necessary to converge on the optimal trajectory (see figure 3). It is important to note that the optimal movement trajectory and joint torques are determined simultaneously. These torques represent muscle force or robotic motor load required to walk on shallow downhill or uphill grades. Leg angles at foot-strike and associated stride-lengths increase monotonically with uphill slope. During downhill walking a passive stability has been observed. However in uphill walking there is no longer passive stability so system resonance disappears. Consequently, during uphill bipedal locomotion there is no natural period to optimize joint torques and the stride period increases to the upper bound allowed by the simulation. Curiously, during level

ground walking and at shallow uphill slopes, i.e. 0.5 deg, the simulation converges upon a bounded stride period. The stance-leg velocity increases monotonically with uphill slope because leg angle increases while stride period was bounded. Swing-leg velocity becomes increasingly negative with slope in response to the hip torque actuation necessary to push the system uphill. Thus, results illustrate that simultaneous solution of movement trajectories and joint actuation in bipedal walking provides sufficient freedom to accurately represent passive dynamic downhill walking or active uphill walking with the a single model.

DISCUSSION

The goal of this effort was to investigate bipedal walking wherein the solution simultaneously established movement trajectories and joint actuation torques to satisfy limit-cycle stability. Most models of biomechanical movement dynamics fully restrict either the movement trajectory or the joint torque actuation. Many biomechanical models of walking employ inverse-dynamic analyses to determine joint torques that strictly describe a-priori movement trajectories. This category of movement simulation is widely used in clinical assessments because modern technology permits easy measurement of multi-segment kinematics. Forward-dynamic simulations represent a second category of simulation wherein movement dynamics are computed based upon pre-specified joint torque profiles. Passive dynamic walkers are a subclass of forward-dynamic models wherein the input torques are assigned to a value of zero. Both forward-dynamic and inverse-dynamic analyses have been used to study walking stability. However, biologic locomotion is rarely limited to fixed behaviors in either movement or joint torque. Instead, both torque and movement are modified and/or compromised to establish a balance in performance. In the trajectory search simulations, the bipedal walking behavior achieved movement trajectories subject to periodicity constraints while joint torque was optimized for minimum input activation and the balance between the two was established through the governing equations of motion. Permitting flexible balance between movement trajectories and actuation torques is necessary to understand potential compensation mechanisms that often occur with pathological disorders in human locomotion.

During downhill walking the movement trajectories converge toward natural passive dynamics to satisfy the energy minimizing objective function. In passive compass-gait, the ground slope

dictates the stable dynamics of the system. Results demonstrate that the forward-integration model and both of the trajectory search simulations generate nearly identical leg angle and velocity profiles that decreased as ground slope approached zero (see figure 2). Simulation output agreed with published simulations of passive dynamic bipedal walking^{6,11,21}. The cause of this behavior can be understood from analyses of system energy. The total energy at the initial time, i.e. immediately following foot-strike of step k, can be represented as

$$E_k = \frac{1}{2} M_H L^2 \dot{\theta}_k^2 + 2M_H gL \sin \theta_k \sin \gamma \quad (16)$$

The first term represents the initial kinetic energy and the second term the potential energy where $L \sin \theta_k \sin \gamma$ represents the location of the system mass above the final position. Although the computer simulation results include both leg mass and HAT mass; for purposes of simplicity equation 16 assumes the leg masses are negligible when compared to the HAT mass. Therefore, at step k+1 the initial energy is

$$E_{k+1} = \frac{1}{2} M_H L^2 \dot{\theta}_{k+1}^2 \quad (17)$$

According to McGeer²¹, as well as equations 1-3 above, the energy transferred from step k (eqn 16) to step k+1 (eqn 17) is decremented by $\cos^2(2\theta_k)$. To assure stability the total initial energy at step k+1 must be identical to the initial energy at step k scaled by the energy loss term at foot strike. Periodicity requires the initial angles and velocities at step k must be equal to step k+1, i.e. $\theta_k = \theta_{k+1} = \theta_i$, for period-one gait¹¹.

$$\frac{1}{2} M_H L^2 \dot{\theta}_i^2 = \left\{ \frac{1}{2} M_H L^2 \dot{\theta}_i^2 + 2M_H gL \sin \theta_i \sin \gamma \right\} \cos^2 2\theta_i \quad (18)$$

Note that energy loss at foot strike is absolutely necessary to achieve stability in passive downhill walking, described by Goswami in terms of the phase-space contraction¹¹. The relation between initial angular velocity and initial leg angle is readily determined. The pendulum frequency of the swing-leg in relation to the range-of motion, $\pm\theta_i$, describes the stride period²¹. The stance-leg must similarly move through a range of $2\theta_i$ in the time period between the swing-leg lift-off and foot-contact. Hence, using small angle approximation, the initial stance-leg velocity is readily determined from the initial leg angle, θ_i , and ground slope, γ .

$$\dot{\theta}_i = \sqrt{\frac{g}{\beta L} \theta_i (\gamma - \theta_i)} \quad (19)$$

where β is the mass distribution ratio, L the leg length, g the gravitational constant. Combining equations 18 and 19, the relation between ground slope and initial leg angle is determined,

$$\gamma = \frac{\theta_i^3}{\theta_i^2 - \beta} \quad (20)$$

This theoretical relationship demonstrates excellent agreement with the more complex computer models that include leg mass. Because energy gain is proportional to ground slope and energy loss is related to the inter-leg angle the initial angle must increase monotonically with steeper ground slope (eqn 20). Substituting this relation into equation 19 it is clear the stance velocity must also increase monotonically with steeper ground slope. Both the forward-integration and trajectory search approaches generated results that agree with these theoretical trends.

Stride period predicted by the simulations demonstrated very little change with ground slope. Stride period at 8° ground slope was only 20 to 25 msec greater than the 0.25° ground slope; a 3% increase. Goswami¹⁰ similarly observed small increases in stride period, approximately 6%, whereas McGeer²² reported a small decrease in stride period with steeper ground slope. Linear approximation from the theoretical analyses (eqns 18-20) suggests the stride period must increase approximately 19 msec over this range of ground slopes, but predict a mean stride period of 784 msec compared with simulation results that averaged 647 to 669 msec depending upon the model design and objective function. This difference in theoretical versus numeric simulation periods is attributable to the simplifying assumptions and linearized representation of the theoretical analyses. Nonetheless, the trajectory search results identified stride periods that were nearly identical to the steady state behavior from forward-integration passive dynamic walking. This natural period represents the resonant frequency of the stable dynamic system. A natural period can also exist during uphill walking but only at very shallow uphill slopes providing the mass distribution ratio, β , in equation 20 is sufficiently large. Otherwise there is no natural period during uphill walking. As a consequence, the solution for uphill walking resulted in stride periods that were bounded by the explicit numeric constraint imposed by the simulation.

During uphill walking there is a clear need for joint torque as a form of input energy (see figure 3). This input torque determined by the objective function and resulted in actuation of both the ankle and hip muscles. However, results demonstrate a clear need for a knee or some other leg lengthening mechanism for uphill walking. To minimize the sum of squared joint torques, both the hip and ankle actuation must be of similar mean amplitude. The difference in average activation between the hip and knee in figure 3 is less than 14%. Recall that hip torques that rotate the stance leg forward have a reaction that will drive the swing leg backward. Consequently, the swing leg demonstrates a large posterior movement early in swing phase. An added degree-of-freedom to permit stance leg extension would allow input energy to the system without introducing this unnatural swing phase behavior. Hopping simulations rely solely upon leg extension energy and may readily travel uphill. Bipedal walking simulations have implemented leg extension mechanisms with success. Camp added powered eccentrically curved feet that worked to actively lift the bipedal walker smoothly throughout stance phase in level ground walking. This inputted potential energy by extending the effective leg length thereby mimicking downhill walking and successfully achieved limit-cycle stability. McGeer²³ examined instantaneous leg lengthening for uphill climbing via analytically methods and concluded that it is most effective when combined with well-timed ankle torque impulses. Future models designed to study dynamic stability in powered bipedal walking must investigate systems with higher degrees-of-freedom.

The trajectory search simulations were constrained to period-one gait behavior. It has been observed that stable passive walking can occur despite stride-to-stride asymmetry. Bifurcation of the natural dynamics may occur, particularly at steep downhill slopes, such that the periodic pattern repeats every second step^{6,11}. Higher-order gait asymmetries may also develop wherein the period repeats every 4 steps, 8 steps, etc. This behavior is strongly influenced by mass distribution of the walker¹¹. For the walker implemented in the current study, 2-period gait patterns were observed at ground slopes in excess of 11°. It remains unknown whether n-period gaits exist during powered or uphill walking. In the trajectory search implementation the periodic behavior was constrained to one-period gait. However, this is not a necessary limitation as advanced simulations could implement these techniques to higher-period behaviors. The search technique was also limited by linear methods requiring a monotonic solution space.

Movement trajectories were seeded at initial leg angles of $\pm 1^\circ$ and separately analyses seeded at $\pm 30^\circ$. Both converged upon similar solution trajectories that agreed with the natural dynamics of the system. Nonetheless it is clear that including the time increment, dt , as a variable produced a nonlinear search space. More advanced trajectory search methods will be required for increasingly complex simulations.

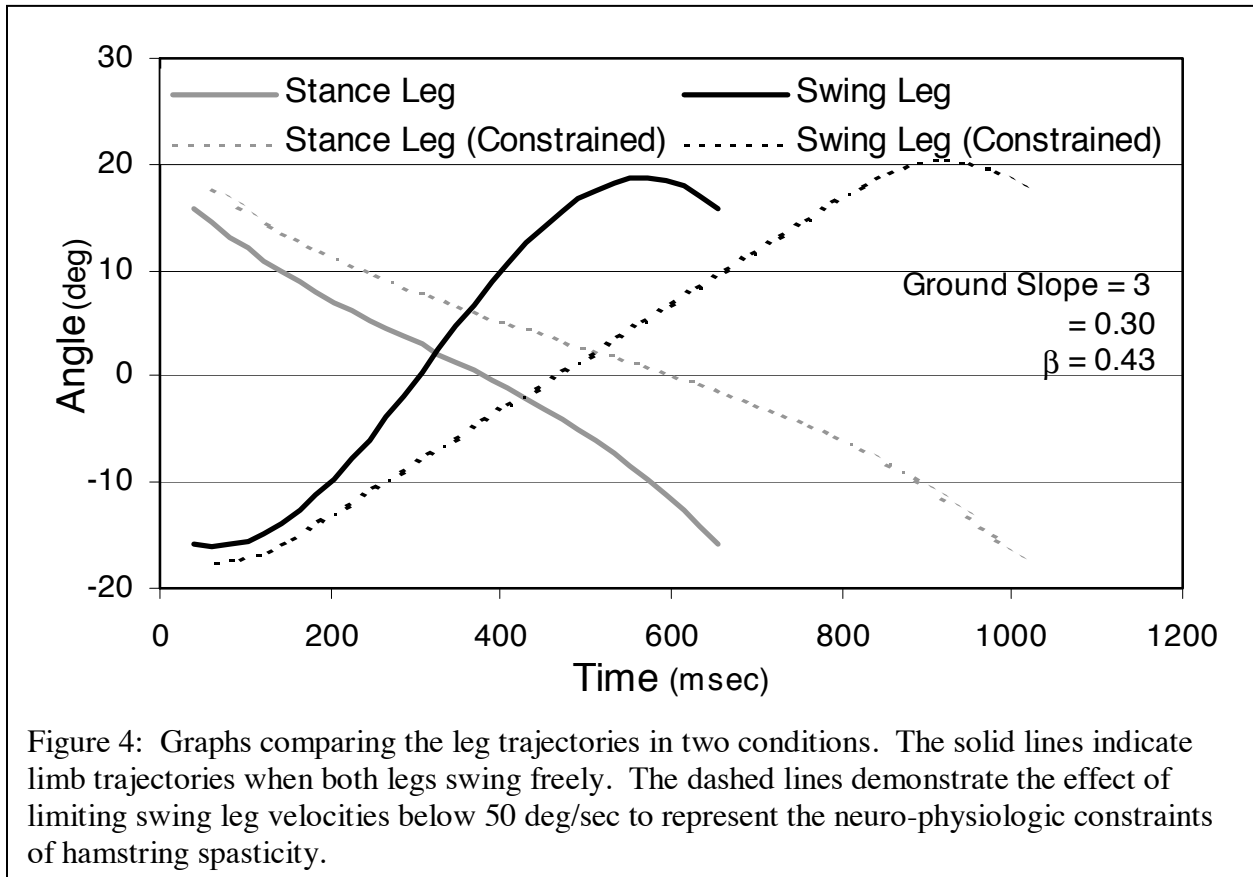


Figure 4: Graphs comparing the leg trajectories in two conditions. The solid lines indicate limb trajectories when both legs swing freely. The dashed lines demonstrate the effect of limiting swing leg velocities below 50 deg/sec to represent the neuro-physiologic constraints of hamstring spasticity.

Impetus for this study is the rhetorical hypothesis that both movement trajectory and joint torque are modulated or adapted to maintain dynamic stability in bipedal walking. Our results with this space-time constraints trajectory search algorithm indicate effective movements and joint torques can be computed for inclined and declined walking tasks. The results of downhill walking are identical to the optimal trajectories specified by the forward-integration approach and the freedom to add constraints permits exploring other tasks. We have investigated uphill walking and pathologic constraints that require non-homogeneous solutions. For example, pathologic behavior was investigated by limiting swing leg velocities below 50 deg/sec to represent the neuro-physiologic constraints of hamstring spasticity¹². The trajectory search walker (see figure

4) produced results that match observations of patients with spastic cerebral palsy, namely increased joint torque was required and stride period was slower thereby modulating both movement trajectory and joint torque in a compensation behavior. To understand pathologic movement dysfunctions the solution set must avoid a priori specification of movement dynamics. Results illustrate that this trajectory search approach to dynamic walking simulation can be implemented to achieve freedom from prespecified motion or torque trajectories yet converge to well-known behaviors of natural dynamics in downhill walking.

ACKNOWLEDGEMENTS

This research was supported in part by a grant HD-99-006-02 from NCMRR of the National Institutes of Health

REFERENCES

1. Alexander R.M. Elastic Mechanisms in Animal Locomotion. Cambridge: Cambridge University Press; 1988:
2. Apkarian J., Naumann S., Cairns B. A three-dimensional kinematic and dynamic model of the lower limb. *J.Biomechanics*. 1989; 22: 143-55.
3. Espiau B. and Goswami A. Compas gait revisited. 1994; Capri, Italy,
4. Garcia M., Chatterjee A., Riuna A., Coleman M. The simplest walking model: Stability, complexity and scaling. *J.Biomech.Eng.* 1998; 120: 281-8.
5. Garcia M., Chatterjee A., Ruina A. Efficiency, speed and scaling of 2D passive dynamic walking. *Dyn.Stabil.Syst.* 2000; 15: 79-99.
6. Garcia M., Ruina A., Coleman M., and Chatterjee A. Passive-dynamic models of human gait. 1996; Mt Sterling, OH,
7. Gilchrist L.A., Winter D.A. A multisegment computer simulation of normal human gait. *IEEE Trans.Rehabil.Eng.* 1998; 5: 290-9.
8. Goswami A., Espiau B., and Keramane A. Limit cycles and their stability in a passive bipedal gait. 1996; Minneapolis, MN,
9. Goswami A., Espiau B., Keramane A. Limit cycles in a passive compass gait biped and passivity-mimicking control laws. *J.Auton.Robots.* 1997;
10. Goswami A., Espiau B., Thuilot B. A study of passive gait of a compas-like biped robot: Symmetry and Chaos. *Intl.J.Robot.Res.* 1998; 17: 1282-301.
11. Goswami A., Thuilot B., and Espiau B. Compas-like biped robot. Part I: Stability and bifurcation of passive gaits. 1996; 2996, INRIA

12. Granata K.P., Damiano D.L., Abel M.F. Joint angular velocity during gait and the influence of muscle-tendon surgery. *J.Bone Jt.Surg.* 2000; 82-A: 174-86.
13. Hemami H., Wyman B.F. Modeling and control of constrained dynamic systems with application to biped locomotion in the frontal plane. *IEEE Trans.Autom.Control.* 1979; AC-24: 526-35.
14. Hodgins J., Raibert M.H. Biped gymnastics. *Intl.J.Robot.Res.* 1990; 9: 115-32.
15. Hurmuzlu Y., Basdogan C, Stoianovici D. Kinematics and dynamic stability of the locomotion of post-polio patients. *J.Biomech.Eng.* 1996; 118: 405-11.
16. Hurmuzlu Y., Basdogan C. On the measurement of dynamic stability of human locomotion. *J.Biomech.Eng.* 1994; 116: 30-6.
17. Hurmuzlu Y., Chang T.H. Rigid body collisions of a special class of planar kinematic chains. *IEEE Trans.Syst.Man Cyber.* 1992; 22: 964-71.
18. Jeng S.F., Holt K.G. Self-optimization of walking in nondisabled children and children with spastic hemiplegic cerebral palsy. *J.Motor Behav.* 1996; 28: 15-27.
19. Kerrigan D.C., Roth R.S., O'Riley P. The modelling of adult spastic paretic stiff-legged gait in swing period based on actual kinematic data. *Gait and Posture.* 1998; 7: 117-24.
20. McGeer T. Passive bipedal running. *Proc.R.Soc.Lond.B.* 1990a; 240: 107-34.
21. McGeer T. Passive dynamic walking. *Intern J.Robot Res.* 1990b; 9: 68-82.
22. McGeer T. Passive walking with knees. 1990; Cincinatti, OH, 1640-1645
23. McGeer T. Dynamics and control of bipedal locomotion. *J Theor Biol.* 1993; 163: 277-314.
24. Onyshko S., Winter D.A. A mathematical model for the dynamics of human locomotion. *J.Biomech.* 1980; 13: 361-8.
25. Pandy M.G., Berme N. Quantitative assessment of gait determinants during single stance via a three-dimensional model. Part I. Pathologic gait. *J.Biomechanics.* 1989; 22: 725-33.
26. Townsend M.A., Seireg A. The synthesis of bipedal locomotion. *J.Biomechanics.* 1972; 5: 71-83.
27. White S.C., Winter D.A. Predicting muscle forces in gait from EMG signals and musculotendon kinematics. *J.Electrophysiol.Kinesiol.* 1993; 2: 217-30.
28. Winter D.A. Biomechanics and Motor Control of Human Movement. 2 ed. New York: Wiley-Interscience Publication; 1990:
29. Witkin A., Kass M. Spacetime Constraints. In Computer Graphics (SIGGRAPH 88), pages 159-- 168. ACM, August 1988.